

A molecular dynamics study of the structural stability of a two-dimensional soft-spheres binary alloy

This article has been downloaded from IOPscience. Please scroll down to see the full text article.

1995 J. Phys.: Condens. Matter 7 2395

(<http://iopscience.iop.org/0953-8984/7/12/004>)

View [the table of contents for this issue](#), or go to the [journal homepage](#) for more

Download details:

IP Address: 171.66.16.179

The article was downloaded on 13/05/2010 at 12:48

Please note that [terms and conditions apply](#).

# A molecular dynamics study of the structural stability of a two-dimensional soft-spheres binary alloy

S Gonçalves†§ and J R Iglesias†||

† Instituto de Física, Universidade Federal do Rio Grande do Sul, Caixa Postal 15051, CP 91501-970 Porto Alegre, RS, Brazil

‡ Laboratoire de Physique des Solides, Université Paris-Sud, Centre d'Orsay, Bâtiment 510, 91405 Orsay, France

Received 31 October 1994, in final form 24 January 1995

**Abstract.** We present molecular dynamics calculations for a two-dimensional binary alloy composed of soft disks. We start the simulation with a system of 108 identical particles at low temperature arranged in a close-packed triangular lattice. Then the diameter ratio  $\lambda$  is varied in steps while the temperature is kept constant. We define a set of order parameters suitable for detecting the existence of ordered binary domains over a wide range of  $\lambda$ -values. The phase diagram thus obtained for the range  $0.3 \leq \lambda \leq 1$  shows two ordered phases: one FCC structure below  $\lambda = 0.5$  and a new structure, not previously reported, for  $0.5 \leq \lambda \leq 0.85$ . This is not expected from Hume-Rothery rules but is in remarkable agreement with experimental results for colloidal systems. Both transitions are first-order ones; we also study hysteresis and metastable states.

## 1. Introduction

It is well known that the mixing of atoms with large differences in atomic size is very unlikely in binary intermetallic compounds, and phase separation is to be expected when the atomic diameters differ by more than 15% [1]. On the other hand, the situation is different in macroscopic systems: in 1980 Sanders [2] found a number of different ordered binary phases of two clearly distinct particle sizes in a natural specimen of gem opal; the components of that sample were silica spheres of diameters 0.36 and 0.21  $\mu\text{m}$ . Recently, Barlett *et al* [3] presented similar results for a manufactured system of bidisperse colloidal particles of radii 0.321 and 0.186  $\mu\text{m}$ . However, there is an important difference between colloidal systems and intermetallic alloys: the long-range attractive force that is absent in the former; but in both studies the authors explained the ordered arrays in terms of packing arguments. Besides the interest in these 'hard-sphere' systems in connection with particle aggregates or the above-mentioned intermetallic compounds, one should consider the possibility of new kinds of material—as suggested by Barlett *et al*—made, for example, by mixing plastic and metallic particles of different sizes.

In a recent work Bocquet *et al* [4] presented numerical simulations of the amorphization of a two-dimensional (2D) binary alloy where particles interact through a soft repulsion potential and molecular dynamics (MD) calculations are performed at constant temperature,

§ E-mail: sgonc@if.ufrgs.br.

|| Permanent address: Instituto de Física, Universidade Federal do Rio Grande do Sul, Caixa Postal 15051, CP 91501-970 Porto Alegre, RS, Brazil.

while the diameters ratio  $\lambda$  ( $\lambda = \sigma_1/\sigma_2$ , where  $\sigma_1$  is the diameter of small particles, 1, and  $\sigma_2$  is the diameter of large particles, 2) is gradually varied, down to a critical value of  $\lambda$  that brings the system into amorphization. Gonçalves *et al* [5] utilized the same procedure to determine the critical value of  $\lambda$  for an interface amorphization in a similar system and found that the interface region transforms into an amorphous state for  $\lambda$ -values a little bigger than for the bulk amorphization of Bocquet *et al*. This could mean that the type of diagnostic technique is decisive in determining whether or not the system attains an ordered phase, and also that images of the system during evolution could be of considerable help.

We present here an attempt to reproduce the dynamics of a bidisperse spheres system, via a MD study of the structural stability of a 2D binary alloy of soft disks, as a function of the size ratio, in order to investigate the existence and formation of ordered mixed structures at small  $\lambda$ -values. In the first part of the calculations we follow the same procedure as in [4] and perform a simulation with 108 identical particles on a triangular lattice, decreasing the size of 54 randomly chosen particles and increasing the diameter of the others. The simulation is performed slowly enough to guarantee the thermodynamic equilibrium of the system throughout the transformation, while particles are moved by MD at constant temperature and volume. Going beyond the transition reported by Bocquet *et al* for  $\lambda = 0.780$ , we find evidence of increasing order in the system for lower values of  $\lambda$ . By direct inspection of the resulting configurations, we observe the formation of domains of binary ordered alloy that looks like some of the structures found by Sanders in the gem opal [2].

In the following we are going to present detailed studies of the emerging structures that give rise to a phase diagram with two ordered phases for small  $\lambda$ -values, separated by a first-order transition for  $\lambda = 0.5$ .

The organization of the work is as follows: in section 2 we present the model and methods; in section 3 we describe the order parameters that we utilize to monitor the transformations; and section 4 is devoted to the results. The conclusions are presented in section 5.

## 2. Model

We consider a 2D model where a fixed number of 'soft disks' interact through a purely repulsive pair potential [4], given by

$$V_{\alpha\beta} = \epsilon \left( \frac{\sigma_{\alpha\beta}}{r} \right)^{12} \quad (1)$$

where  $\epsilon$  sets the energy scale and  $r$  is the distance between centres of a pair of interacting disks.  $\sigma_{\alpha\beta}$  is the 'distance' between two disks in contact, and is defined as

$$\sigma_{\alpha\beta} = \frac{1}{2}(\sigma_\alpha + \sigma_\beta) \quad \alpha, \beta = 1, 2. \quad (2)$$

In the simulations that we are going to describe in section 4.1 we consider a hexagonal box with  $N$  close-packed disks arranged on a perfect triangular lattice. Six replicas of the central box are considered at each side of the hexagon to guarantee the periodic boundary conditions. Then one chooses at random  $N/2$  disks and decreases their diameter,  $\sigma_1$ , while increasing  $\sigma_2$ , that of the  $N/2$  remaining disks and keeping constant the mean atomic diameter  $\sigma$  defined, according to conformal solution theory [6], as

$$\sigma^2 = x_1^2 \sigma_{11}^2 + 2x_1 x_2 \sigma_{12}^2 + x_2^2 \sigma_{22}^2 \quad (3)$$

which is equal to the initial value  $\sigma$  of the monodisperse system;  $x_i$  is the concentration of the species  $i$ , so in this case  $x_1 = x_2 = 0.5$ .

The size ratio of the two kinds of particle in the system is denoted by the parameter

$$\lambda = \frac{\sigma_1}{\sigma_2} \leq 1. \quad (4)$$

So, the excess (with respect to an ideal gas) thermodynamic properties of a soft-disk bidisperse system in equilibrium depend only on  $\lambda$ , the concentrations  $x_i$  and on the dimensionless constant

$$\gamma = \frac{N\sigma^2}{S} \left( \frac{\epsilon}{k_B T} \right)^{1/6} \quad (5)$$

where  $N\sigma^2/S$  and  $k_B T/\epsilon$  play the role of reduced number density and temperature, respectively [7],  $k_B$  being the Boltzmann constant and  $S$  the area of the box. The melting point for the monodisperse ( $\lambda = 1$ ) system corresponds to  $\gamma \cong 1$  [8].

The time unit of the simulations is  $\tau = \sqrt{m\sigma^2/\epsilon}$ , where  $m$  is the mass of the particles, and the time step  $\Delta t = 5 \times 10^{-3} \tau$ . All the simulations are carried out for a fixed number of particles  $N$  and fixed concentration,  $N_i = N/2$ ; thus the density of the system remains constant. The temperature is held constant by means of the thermostat of Hoover *et al* (see [9]) in the variant of the leap-frog scheme proposed by Brown and Clarke [10]. Consequently each complete simulation corresponds to a fixed value of  $\gamma$ , while  $\lambda$  is the sole free parameter.

### 3. Order parameters

When  $\lambda$  decreases from the perfect-crystal initial condition value ( $\lambda = 1$ ) the system evolves towards a binary configuration with some degree of disorder, which may lead to a phase transition. To monitor the order-disorder transition one can employ different order parameters that are defined as follows [4].

(i) The structure factor, that is a measure of the translational order,

$$\rho_G = \left\langle \frac{1}{N} \left| \sum_i \exp(i\mathbf{G} \cdot \mathbf{R}_i) \right|^2 \right\rangle \quad (6)$$

where  $\mathbf{R}_i$  specifies the position of atom  $i$  and  $N$  is the total number of atoms in the system. Hereafter  $\langle \dots \rangle$  denotes an ensemble average. The structure factor  $\rho_G$  is evaluated for a given reciprocal-lattice vector  $\mathbf{G}$  of the triangular lattice;  $\rho_G = 1$  for a perfectly ordered periodic lattice, and decreases as  $1/\sqrt{N}$  for a disordered system.

(ii) Another measure of the degree of translational order is the mean square displacement ( $\Delta^2 r$ ), given by

$$\langle \Delta^2 r \rangle = \frac{1}{N} \sum_{i=1}^N \langle (\mathbf{R}_i - \mathbf{R}_{i0})^2 \rangle \quad (7)$$

where  $\mathbf{R}_{i0}$  specifies the lattice position of atom  $i$ . Thus,  $\langle \Delta^2 r \rangle$  is a measure of the displacement of the atoms from their zero-temperature equilibrium positions.

(iii) The bond-orientation order is evaluated from the order parameter of Nelson and Halperin [11]:

$$\langle \Psi_{ij} \rangle = \frac{1}{N} \sum_{i=1}^N \left\langle \left| \frac{1}{n_i} \sum_{j=1}^{n_i} e^{i6\theta_{ij}} \right|^2 \right\rangle \quad (8)$$

where  $n_i$  is the number of nearest neighbours of the atom  $i$ , and  $\theta_{ij}$  is the angle formed by the bond of an  $(i, j)$  pair of nearest neighbours with respect to a fixed polar angle.  $\langle \Psi \rangle = 1$  for a perfect triangular crystal, and goes to zero as the local disorder increases.

(iv) Finally one can compute the fraction of atoms having exactly six neighbours,  $f_6$ , by counting the number of particles within a cut-off radius  $r_c$  lying midway between nearest and next-nearest lattice positions, and given by

$$f_6 = \frac{1}{N} \left\langle \sum_{i=1}^N \delta_{n_i,6} \right\rangle. \quad (9)$$

This method is much easier and faster to perform than the Voronoi construction and seems to be equivalent to it, at least for the dense fluid phase near freezing and in the solid-state phase [8]. However, one should take care with it when  $\lambda$  is far from 1, as it will be seen in section 4.2.

Each order parameter is computed separately for each set of particles (small ones and large ones). Then  $\rho_G^i$  denotes the  $\rho_G$  order parameter evaluated over atoms of species  $i$  ( $i = 1, 2$ ). The same is valid for the  $\langle \Delta^2 r \rangle$  order parameter. For the Nelson–Halperin [11] order parameter we consider three types of bond:  $\langle \Psi_{11} \rangle$  for bonds between type 1 atoms,  $\langle \Psi_{22} \rangle$  for those between type 2 atoms, and  $\langle \Psi_{12} \rangle$  for mixed bonds. Finally, in the evaluation of  $f_6^i$  one just considers the number of neighbours, independently of the kind.

Moreover, one can obtain supplementary information from the average atomic positions and the pressure as functions of the atomic size ratio  $\lambda$ . It can be shown that the pressure and the Helmholtz free energy differ only by a constant factor in systems with a power-law interaction potential; thus we will consider them as equivalent magnitudes. We have verified that the pair correlation functions, another common way of measuring the order in the system, do not give additional information, so we do not discuss those results here.

## 4. Results

### 4.1. Hexagonal box

In [4], the atomic size ratio,  $\lambda$ , varies from 1—a monodisperse perfect triangular structure—to 0.7 ( $\gamma$  fixed at 1.64), and a first order phase transition is obtained for  $\lambda = 0.78$ , to a configuration that is described as an amorphous one. In this section we perform the same kind of calculation and reproduce the phase transition for the same critical value of the size ratio, although we vary  $\lambda$  quite a lot faster than was done in [4]. The simulations are performed starting with a monodisperse system, characterized by  $\lambda = 1$ , and then slowly reducing the size ratio to values of  $\lambda$  below 1, in a sequence of steps of  $\delta\lambda = 10^{-5}$ . After every step we let the system stabilize at constant  $\lambda$  for 400 time steps  $\Delta t$ . This process is repeated up to an accumulated variation of  $\Delta\lambda = 500\delta\lambda$ , when the statistical averages reported below are computed over a period of 2000  $\Delta t$  at a fixed value of  $\lambda$ . The whole procedure is repeated until the desired value of  $\lambda$  is achieved. Finally, in order to understand the above-mentioned experimental results we push the limiting value of  $\lambda$  far beyond  $\lambda = 0.78$  and find indications of a new transition to an ordered state.

The results are presented in figure 1, where we plot the order parameters  $f_6^1$ , the fraction of small atoms having six neighbours, and  $f_4^1$ , the fraction of small atoms having four neighbours, as functions of  $\lambda$ . For  $1 \geq \lambda \geq 0.78$ ,  $f_6^1 = 1$ , which characterizes a perfect triangular lattice. Going down from  $\lambda = 0.78$  the ordered phase starts to disappear, corresponding to the first-order transition reported by Bocquet *et al* [4]. When  $f_6^1$  attains a value near  $f_6^1 = 0.2$ , this order parameter does not give further information and the system

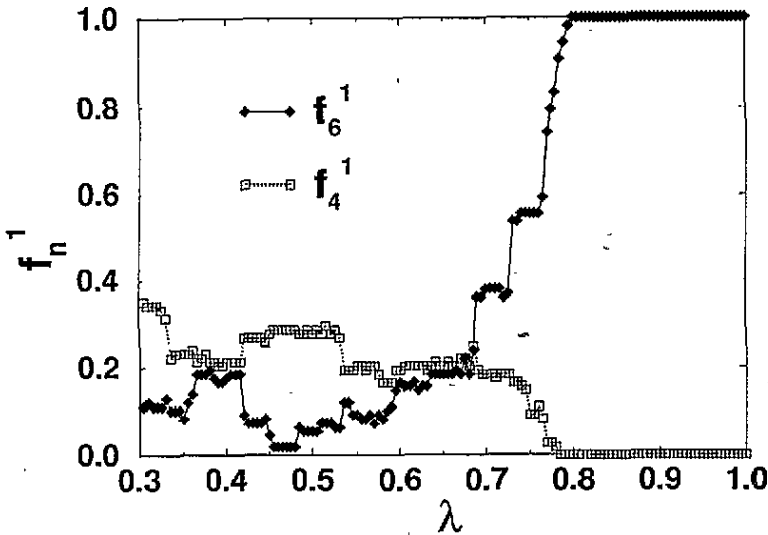


Figure 1. The fraction of small particles having exactly six neighbours,  $f_6^1$ , and the fraction of small particles having exactly four neighbours,  $f_4^1$ , versus  $\lambda$  for a transformation from  $\lambda = 1$  to  $\lambda = 0.3$ , in a hexagonal box for  $\gamma = 1.64$ .

seems to be in an amorphous state. However, supplementary information can be obtained from  $f_4^1$ , which starts to increase from zero, for the same value of  $\lambda = 0.78$ . Immediately after the transition one finds roughly the same number of atoms with six neighbours and four neighbours, but at the end of the transformation ( $\lambda = 0.3$ ) 10% of the particles have six neighbours, while more than 30% have four. This is a clear indication that an arrangement where each site has four neighbours is more stable than a six-neighbours one.

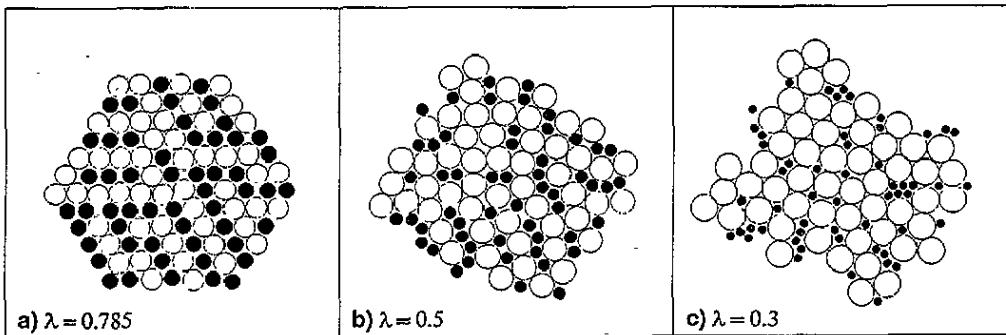
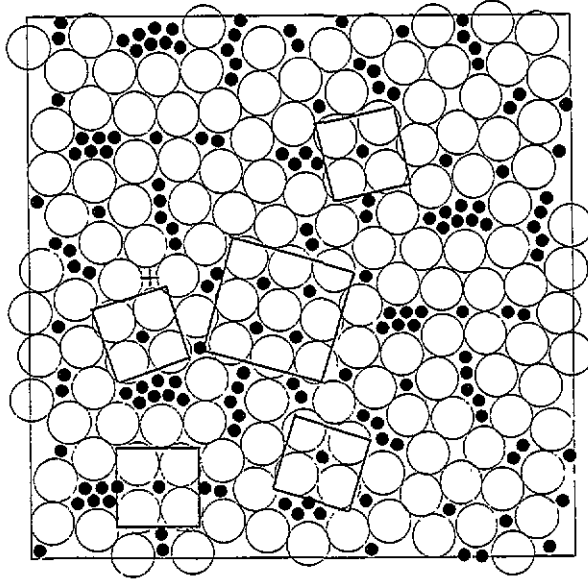


Figure 2. Snapshots of the averaged particle positions for  $\lambda =$  (a) 0.785, (b) 0.5 and (c) 0.3 for a transformation from  $\lambda = 1$  to  $\lambda = 0.3$  in a hexagonal box for  $\gamma = 1.64$ .

In figure 2 we present a sequence of 'snapshots' of the system for different values of  $\lambda$  from 1 to 0.3. One can see that the lattice is still a triangular one for  $\lambda = 0.785$  (figure 2(a)), while it shows an 'amorphous' state for  $\lambda = 0.5$  (figure 2(b)), i.e. atoms with four, five and seven neighbours are clearly seen; finally, for  $\lambda = 0.3$ , it is possible to identify a domain of considerable size (13 atoms) that corresponds to a perfect binary alloy (figure 2(c)). Notice the continuous change of shape of the cluster of particles inside the dynamic box, that starts as a hexagon and ends approximately as a square. This is not a simulation artifact, for we

have maintained hexagonal periodic boundary conditions throughout the process.



**Figure 3.** As figure 2(c) but complemented with periodic replicas, showing marked ordered domains, clusters of small particles, a domain of perfect triangular large particles and a group of four large atoms with a vacancy of a small atom, denoted with a cross.

Figure 3 shows the final configuration for  $\lambda = 0.3$ , complemented with periodic boundaries and where we have stressed the domains of perfect binary alloy. The structure of these domains looks like some of the configurations found by Sanders for the gem opal [2]. One can see clusters of small atoms and domains of perfect triangular lattices of large ones too, and also a square configuration of four large atoms with a vacancy of a small one (marked with a cross). From these results it is difficult to decide whether the system is in an amorphous state after the transition, and there are no signs of particle segregation. On the other hand, there is a trend towards binary mixing for low values of  $\lambda$ .

### 5. Square box

Now we take the opposite point of view and consider as the starting point a perfect binary alloy of 100 particles (50 small and 50 large) in a square box with  $\lambda = 0.3$  (and periodic boundary conditions), arranged—as in the emerging domain of figure 3—in a 2D NaCl structure, with  $\gamma$  fixed at 1.59. This is a slightly different value from the  $\gamma = 1.64$  of the previous section and of [4] due to the density difference between the square and the hexagonal structures. Nevertheless we have verified that this difference does not modify the critical parameters of the phase transitions.

We present in figure 4 a snapshot of the system in the initial configuration, which we call the  $\alpha$ -phase. The aim is now to investigate the stability of the system from the  $\alpha$ -phase to a monodisperse configuration when increasing  $\lambda$  from  $\lambda = 0.3$  to  $\lambda = 1$ , considering the same order parameters presented in section 3 but adapted to a square lattice, in order to detect the structural changes in the  $\alpha$ -phase.

In figure 5 we exhibit four order parameters: the structure factor  $\rho_G$ , where  $G$  is a reciprocal-lattice vector of a square lattice, the mean square displacement ( $\Delta^2 r$ ) relative

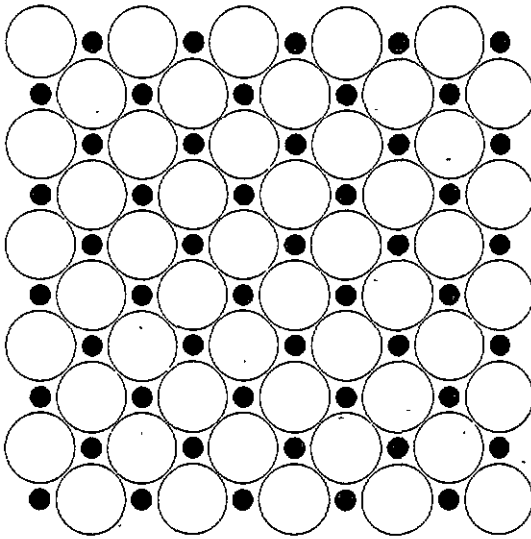


Figure 4. A picture of the initial  $\alpha$ -phase system configuration at  $\lambda = 0.3$ , in a square box and for  $\gamma = 1.59$ .

to the  $\alpha$ -phase lattice positions, the Nelson-Halperin order parameter  $\langle \Psi_{1j} \rangle$  of a square structure (i.e. changing 6 to 4 in the exponential function of (8)), the fraction of atoms having exactly four neighbours  $f_4$  and the pressure as functions of  $\lambda$ . All of these, with the exception of  $f_4$  (figure 5(d)), exhibit sharp discontinuities at  $\lambda = 0.5$  and  $\lambda = 0.85$ . One interesting point concerning the transition for  $\lambda = 0.5$  is the simultaneous jump of the order parameters  $\rho_G$  and  $\langle \Delta^2 r \rangle$ , corresponding to the disappearance of the long-range translational order (figures 5(a) and 5(b)), while  $\langle \Psi_{11} \rangle$ , the bond-orientation order parameter for pairs of small particles, exhibits a rapid increase (from a zero value), indicating a new configuration with a different order of local orientations (figure 5(c)).

On the other hand the order parameters related to the large (type 2) atoms  $\Psi_{22}$  and  $f_4^2$  fail to detect the  $\alpha$ - $\beta$  transition (figure 5(c) and 5(d)). The orientation parameter  $\Psi_{22}$  substantially increases after the transition, exhibiting large fluctuations and, according with  $f_4^2$ , the transition looks like a second-order one. Both results indicate that the cut-off radius  $r_c = 1.2$  (in units of the first-neighbour distance of the initial  $\lambda = 0.3$  configuration) may be inappropriate. In fact, performing a test with a  $r_c = 1.3$ , the order parameters lead to a sharp first-order transition for  $\lambda = 0.5$ . The original choice of  $r_c = 1.2$  was made on the basis of [8], as the author stated that  $r_c$  between first and second neighbours is equivalent, within 5%, to Voronoï construction; but the present calculation verifies that this is not the case in a bidisperse system with very different diameters.

Hence, we have performed an evaluation of the coordination numbers (for type 1 and type 2 atoms separately) using the Voronoï construction over the averaged configurations stored every  $2 \times 10^5$  time steps. The coordination numbers are sensitive to the two transitions but they assign the same value (six) to the  $\alpha$ -phase as to the triangular lattice ( $\lambda > 0.85$ ). The difficulty here with the characterization of the  $\alpha$ -phase arises from the degeneracy of the square array. Actually, thermal vibrations remove the degeneracy and the Voronoï construction identifies six edge polygons, assigning two second neighbours to each particle in the lattice.

So the choice of the order parameters appropriate for characterizing the transitions is



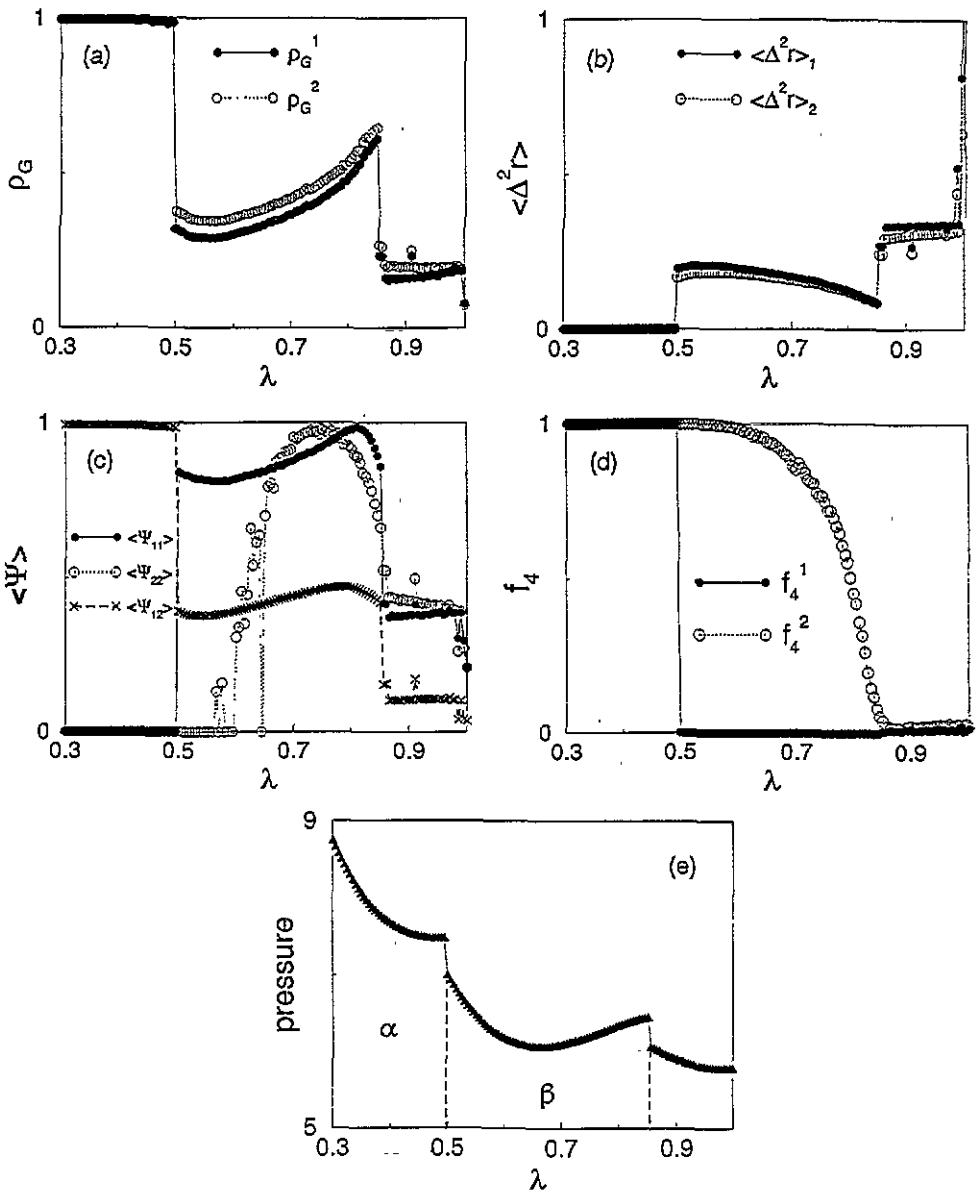


Figure 5. Order parameters and pressure versus size ratio  $\lambda$  for a square box. Transformation from  $\lambda = 0.3$  to  $\lambda = 1$  for  $\gamma = 1.59$ . (a) Structure factor  $\rho_G$ , (b) mean square displacement ( $\Delta^2 r$ ), (c) Nelson-Halperin order parameter ( $\Psi$ ), (d) fraction of atoms having exactly four neighbours  $f_4$ , and (e) pressure. In (a), (b) and (d) the index 1 refers to small particles, while index 2 refers to large particles. In (c), index 11 means bonds between small particles while index 22 means bonds between large ones, and index 12 refers to mixed bonds.

delicate. Here we choose to work with a rather redundant set of order parameters and it is obvious that additional diagnostics *a posteriori* over the stored averaged configuration are always possible. Finally, direct inspection of the snapshots can provide very useful guides.

Coming back to the phase transition for  $\lambda = 0.5$ , figure 6 illustrates the configuration of the system for that value of  $\lambda$ , where a new ordered configuration is apparent. This

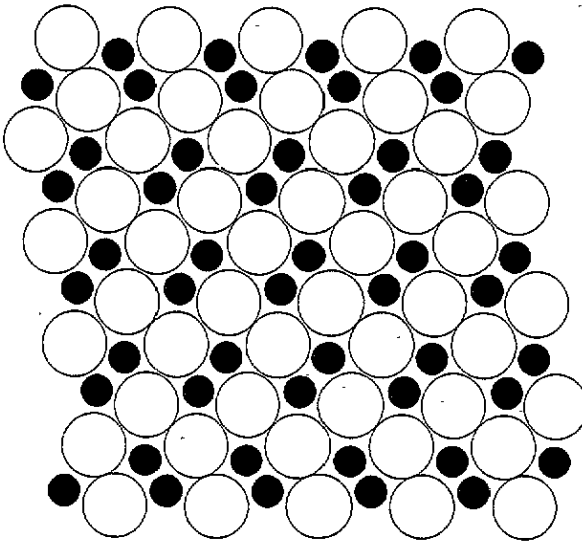


Figure 6. A snapshot of the averaged particle positions for  $\lambda = 0.5$  ( $\beta$ -phase configuration) for the transformation from  $\lambda = 0.3$  to  $\lambda = 1$ , in a square box and for  $\gamma = 1.59$ .

phase is characterized by presenting pairs of small particles disposed in parallel, equally spaced, lines. In these lines all pairs have the same orientation ( $\cong 45^\circ$  relative to the [10] direction), and from line to line the pairs are oriented almost perpendicularly. Thus, we have found a new structure, a superlattice (hereafter referred as a  $\beta$ -phase), with the same lattice parameter, along the [10] direction, as the  $\alpha$ -phase structure, while along the [01] direction the lattice parameter can be two or more times the original one (according to the change in the pair orientation from line to line).

This result is not an artifact of the simulation, as will be verified from the energy calculation, but also the similarities between this 2D  $\beta$ -phase and some patterns of the ordered structures of the gem opal obtained by Sanders [2] are dazzling. Particularly, the size ratio that Sanders measures is well inside the range of values of  $\lambda$  corresponding to the  $\beta$ -phase.

We have performed additional runs with different numbers of particles, to check the dependence of the results on the size of the sample. From  $N = 64$  up to  $N = 256$  one obtains the same qualitative results with minor variations of the critical value of  $\lambda$  ( $\lambda = 0.485$ – $0.500$ ). However, the sequence of angle inclinations from line to line changes with size, whereas the value of the free energy per particle does not show any appreciable difference. This means that the energy associated with different pair orientations from one line to the other is very low, but certainly the two configurations are separated by a high energy barrier. A particular aspect of these new structures is that the orientation order of the pairs increases from the transition point,  $\lambda = 0.5$ , up to a maximum value for  $\lambda = 0.81$ , detected by the orientation order parameter  $\langle \Psi_{11} \rangle$ . At this point the system undergoes a new phase transition to a state that looks like an amorphous one for a value of  $\lambda = 0.85$ . Both transitions ( $\lambda = 0.5$  and  $\lambda = 0.85$ ) can be clearly identified by any of the order parameters utilized except  $f_4$ , but  $\langle \Psi_{11} \rangle$  is the one that gives the most complete information, and is the only one that detects the order of the  $\beta$ -phase. As these diagnostics are especially suited for a square lattice, we cannot utilize them to differentiate between an amorphous state and a triangular lattice. However, by direct inspection of the corresponding snapshot (figure 7),

one can say that the amorphous state is actually an almost triangular lattice with defects, a grain boundary being the most visible one.

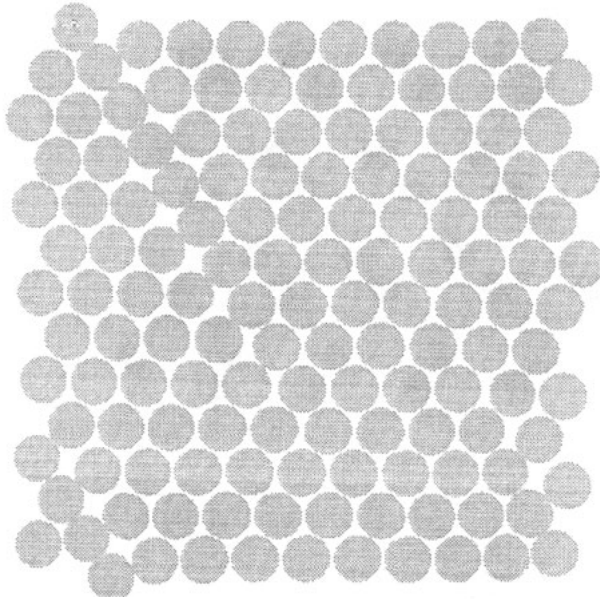


**Figure 7.** A snapshot of the averaged particle positions for  $\lambda = 1$  (monodisperse system) after the transformation from  $\lambda = 0.3$  ( $\alpha$ -phase), in a square box for  $\gamma = 1.59$ . In order to visualize the grain boundary look at the picture at a small angle while rotating it.

Now we focus our attention on the vicinity of  $\lambda = 0.85$  to look at the  $\beta$ -‘amorphous’ transition. We recall that the transition from a triangular lattice to an amorphous configuration, reported by Bocquet *et al* [4], occurs at  $\lambda = 0.78$ ; therefore the difference between these values is a strong indication of the hysteresis of this first-order transition. In fact the ‘amorphous’ state reported in [4] is just a metastable state, for values of  $0.5 \leq \lambda \leq 0.85$ , of higher energy than the corresponding minimum-energy configuration: the  $\beta$ -phase. Also, the amorphous configuration obtained in the present calculation for  $\lambda \geq 0.85$  is a metastable state, whereas the perfect triangular lattice is the minimum-free-energy configuration. The width of this hysteresis cycle, and the required time for the system to go from a metastable configuration to the minimum energy one, will be discussed below.

## 6. Hysteresis

In order to perform a deeper examination of the hysteresis of the transition, we take the final ‘amorphous’ metastable state obtained when going from  $\lambda \approx 0.3$  to  $\lambda = 1$  as the starting configuration (figure 7) and perform the transformation in size ratio back to  $\lambda = 0.3$ . Now, no evidence of a first-order transition is found either for  $\lambda \approx 0.85$  or for  $\lambda = 0.78$ . The transition for  $\lambda = 0.78$  is not observed because the system is already disordered from the beginning ( $\lambda = 1$ ). Neither is the reverse transition, at  $\lambda = 0.85$ , between the disordered state and the  $\beta$ -phase achieved, even for lower values of  $\lambda$ , and this is a indication of the large hysteresis of the transition. The system remains in a disordered state while the minimum-energy one is the ordered  $\beta$ -phase. A high energy barrier separates the local

minima of the free energy of the two configurations. Figure 8 confirms this hypothesis: it shows the pressure versus  $\lambda$  for the present transformation (from  $\lambda = 1$  to  $\lambda = 0.3$ ) as well as for the previous one (from  $\lambda = 0.3$  to  $\lambda = 1$ ). The latter exhibits a discontinuity at the transition, while the former is smooth. The curve intersects for  $\lambda = 0.8$ , indicating the coexistence of the phases, but an energy barrier frustrates the transition and the system remains in a disordered configuration down to  $\lambda = 0.3$ , always with an energy greater than that corresponding to the  $\beta$ - or  $\alpha$ -phases. As the simulations have been performed at 'low temperatures', a considerable amount of time would be necessary to observe the jump from the metastable disordered configuration to the ordered phase. In order to bypass this problem we employed the following procedure: one takes as a starting point the metastable configuration for  $\lambda = 0.35$  at low temperature ( $\gamma = 1.59$ ) (this configuration is the result of going from the  $\alpha$ -phase ( $\lambda = 0.3$ ) to  $\lambda = 1$  and back to  $\lambda = 0.35$ ); then the temperature of the system is slowly increased, keeping  $\lambda$  constant. At a temperature that corresponds to  $\gamma = 1.13$  we observe a small jump in one order parameter and a corresponding one in the pressure, as is shown in figure 9. Then, decreasing the temperature to the initial value of  $\gamma = 1.59$ , it is evident that the free energy of the system has decreased (figure 9). A picture of the system after the thermal treatment is shown in figure 10 where one can observe a great variety of structures: a relatively big domain of  $\alpha$ -phase is well apparent, besides some clusters of small atoms, pairs of them and domains of big atoms with perfect triangular order. It is remarkable that this heterogeneous structure with domains of  $\alpha$ -phase returns the memory of the  $\alpha$ - $\beta$  transition: if one increases  $\lambda$  once again one can retrieve jumps in the order parameters for  $\lambda = 0.5$ ; the critical size ratio of the phase transition remains fixed in this mixed system, but the magnitude of the jumps is reduced because just a fraction of the system—the  $\alpha$  domain—undergoes it.

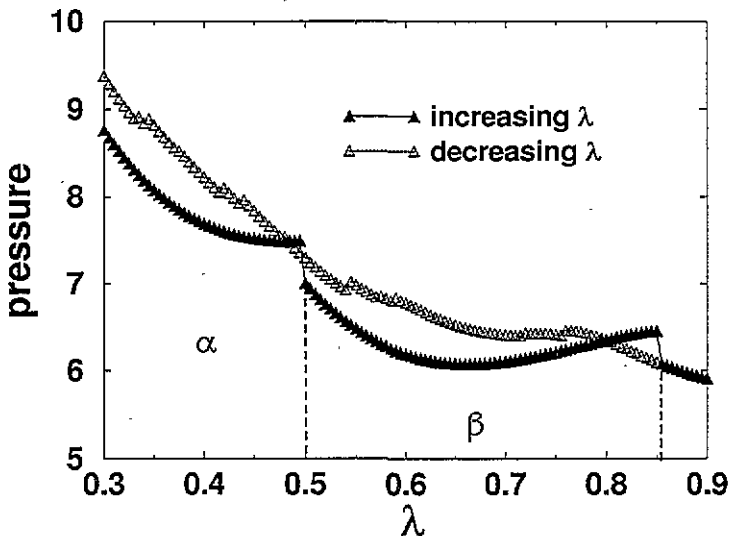


Figure 8. The hysteresis of the transformation: pressure versus  $\lambda$  for the transformation from  $\lambda = 0.3$  to  $\lambda = 1$  and the inverse transformation from  $\lambda = 1$  to  $\lambda = 0.3$ , in a square box for  $\gamma = 1.59$ .

This partially ordered structure may still be 'improved' by means of extra thermal peaks but we want to point out that the constant-temperature algorithm is perhaps not the best way to do that. As a matter of fact for each temperature the system has to be subjected

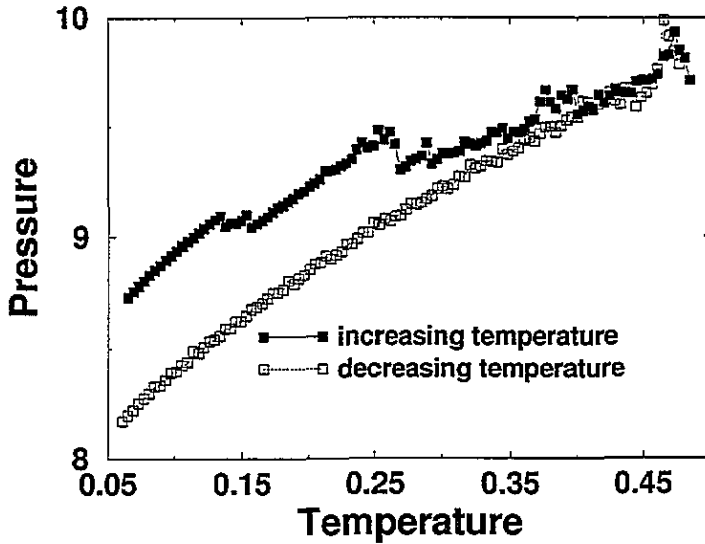


Figure 9. Thermal treatment of the metastable configuration for  $\lambda = 0.35$ : pressure versus temperature for the metastable configuration obtained after a forth-and-back run for a  $\lambda$ -transformation, starting from the  $\alpha$ -phase at  $\lambda = 0.3$  in a square box. The temperature is increased from 0.06 ( $\gamma = 1.59$ ) to 0.48 ( $\gamma = 1.13$ ) and then decreased to 0.06 with  $\lambda$  fixed at 0.35. The pressure is in units of  $\epsilon/\sigma^2$  and the temperature is measured in units of  $\epsilon/k_B$ .

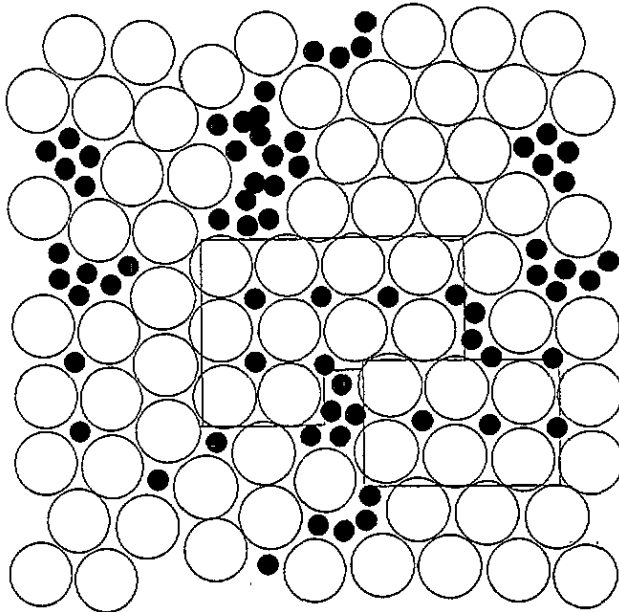


Figure 10. An averaged snapshot (complemented with periodic replicas) for the metastable configuration, for  $\lambda = 0.35$  and  $\gamma = 1.59$ , after the thermal treatment, showing domains of  $\alpha$ -phase (two of them marked with solid lines) and clusters of small and big particles.

to the constant-temperature constraint, so no thermal fluctuations are permitted at any time. This constraint may be too strict: the system does not have enough chances to explore the

phase space—particularly when it has a rich structure of hills and valleys. It is possible that if the constant-temperature constraint is relaxed, or substituted for with a more efficient algorithm, one would get some improvements in the evolution of the system towards an ordered structure. Work is in progress in this direction.

## 7. Conclusions

We have presented here a molecular dynamics simulation of a two-dimensional binary alloy of as much as one hundred soft-disk particles. We have obtained an order–disorder transition at the same value of  $\lambda$  as in the work of Bocquet *et al* [4] but also a completely new result, the  $\beta$ -phase, a superstructure that is stable between the values of  $\lambda = 0.5$  and  $\lambda = 0.85$ , and that has not been observed before in simulations. Also, in spite of the fact that the simulation is performed in 2D, with a simple model potential and a relatively low number of particles, the results are in good agreement with recent and very promising experiments on bidisperse colloidal systems, even from a quantitative point of view. Unexpectedly, periodic boundary conditions show no influence on the results, i.e. the  $\alpha$ -phase domains for small  $\lambda$  values appear both in the square box and the hexagonal box. As a consequence, we think that workable simulations can be of great help in connection with real experiments despite the apparently insurmountable gap between the corresponding time scales. As a final remark let us say that still ‘better’ configurations can certainly be obtained within reasonable computing times using more efficient algorithms, and in this way one might give useful hints for the experimental counterpart, such as annealing techniques.

## Acknowledgments

One of us (SG) acknowledges stimulating discussions with Dr G Martínez. We acknowledge the Centro de Supercomputação da Universidade Federal do Rio Grande do Sul for computing time at the CRAY Y-MP2. We acknowledge the support of CNPq (Conselho Nacional de Desenvolvimento Científico e Tecnológico, Brazil), CAPES (Coordenação de Aperfeiçoamento de Pessoal de Nível Superior—Ministério da Educação e do Desporto, Brazil) and FAPERGS (Federação de Amparo à Pesquisa do Estado de Rio Grande do Sul, Brazil). One of us (JRI) would also like to acknowledge the European Economic Community (EEC) and the Laboratoire de Physique des Solides of the Université Paris-Sud for support and hospitality during the final stages of this work.

## References

- [1] Hume-Rothery W, Smallman E R and Haworth C W 1969 *The Structure of Metals and Alloys* (London: The Metals and Metallurgy Trust)
- [2] Sanders J V 1980 *Phil. Mag.* A 42 705
- [3] Barlett P, Ottewill R H and Pusey P N 1990 *J. Chem. Phys.* 93 1299; 1992 *Phys. Rev. Lett.* 68 3801
- [4] Bocquet L, Hansen J P, Biben T and Madden P 1992 *J. Phys.: Condens. Matter* 4 2375
- [5] Gonçalves S, Ramírez R and Kiwi M 1994 *J. Phys.: Condens. Matter* 6 4213
- [6] Leland T W, Rowlinson J S and Sather G A 1968 *Trans. Faraday Soc.* 64 1447
- [7] Hoover W G, Ross M, Johnson K W, Henderson D, Baker J A and Brown B C 1970 *J. Chem. Phys.* 52 4931
- [8] Broughton J Q, Gilmer G H and Weeks J D 1982 *Phys. Rev. B* 25 4651
- [9] Hoover W G 1983 *Physica A* 118 111
- [10] Brown D and Clarke J H R 1984 *Mol. Phys.* 51 1243
- [11] Nelson D R and Halperin B I 1980 *Phys. Rev. B* 21 5312